BONE REMODELING BASED ON CELLS ACTIVITIES AND PHARMACOKINETICS

Miguel Tobias Bahia

migueltbahia@ifsc.edu.br

Instituto Federal de Santa Catarina

Rua Pavão, 1377, Costa e Silva, CEP 89220-618

Mildred Ballin Hecke

mildredhecke@gmail.com

Universidade Federal do Paraná

Emilio Graciliano Ferreira Mercuri

mercuri@ufpr.br

Universidade Federal do Paraná

Bairro Jardim das Américas, Curitiba - PR, Brasil

Abstract. *This work presents a pharmacokinetic model for antiresorptive agents integrated to a bone remodeling model based on the behavior of bone cells populations. The proposed pharmacokinetic model describes the time course of drug in bone and is physiologically based (PBPK). The bone tissue is modeled by two compartments: one metabolically active, where the remodeling process acts, and another metabolically inactive, which does not undergo remodeling. The simulation of bone remodeling is developed through a dynamic model of bone cells populations in which the temporal evolution of cells like osteoblasts, osteoclasts and the bone volume is governed by a system of differential equations. The system is solved by the 4th order Runge-Kutta method and all procedures were implemented in Matlab. Preliminary results indicate that the model is able to reproduce the expected action of antiresorptive agents on the temporal evolution of bone cells populations. According to the drug dose, route and frequency of administration, the procedure implemented allows to adjust the bone remodeling process.*

Keywords: *Bone remodeling, Pharmacokinetics, Bone cells, Mathematical modeling*

1 INTRODUCTION

Bone remodeling is a physiological process of bone adaptation in response to metabolic or mechanical stimuli. At the cellular level, remodeling process involves primarily osteoblast-mediated bone formation and osteoclast-mediated bone resorption.

The approaches adopted for numerical simulation of bone remodeling can be quite different. Among them the following methods can be cited: essentially mechanistic, phenomenological, multiscale, optimization or even those based on hybrid techniques (Rieger, 2011).

The mathematical models for bone remodeling based on the dynamics of cellular populations correspond to a rather recent research area. Among the pioneering works, we can highlight the work of Kroll (2000), which analyzes the dual action of the parathyroid hormone (PTH) on bone formation and resorption and the work of Komarova et al. (2003), that models the autocrine and paracrine interactions between osteoblasts and osteoclasts. Lemaire et al. (2004) explicit the participation of signaling molecules like OPG, RANKL and PTH. Based on the Lemaire et al. (2004) model, Pivonka et al. (2008) rewrites the signaling expressions using activation and repression functions from chemical kinetics (Hill functions) and incorporates other molecular signaling into the model. In addition, Scheiner et al. (2013) combines the Pivonka et al. (2008) model with the continuum micromechanics and incorporates the mechanical stimulus evaluated in the microscale using a Mori-Tanaka homogenization squeme (Mori and Tanaka, 1973).

Considering the social relevance of bone diseases studies, several mathematical models for bone remodeling have been used to recreate scenarios that include the therapeutic action of medications. Simulation with pharmacological models offers new possibilities to be explored. Parameters such as drug dose, frequency and route of administration may be included in the model, which would make the simulation quite relevant in the aspect of treatment analysis, prevention and cure of bone diseases.

The association of dynamical models of bone cells populations with pharmacological models has occurred in few studies. For instance, the works of Scheiner et al. (2014) and Hambli et al. (2016) incorporate a pharmacokinetic model for Denosumab, a drug used for the treatment of osteoporosis, into the models of Pivonka et al. (2008) and Komarova et al. (2003), respectively.

The most commonly adopted approach for pharmacological models of drugs is the representation of the body as a system of compartments, which are imaginary units (without anatomical or physiological reality) to represent groups of tissues with similar drug distribution rates.

Physiologically based pharmacokinetics models (PBPK) also use tissue or organ representation with compartments but incorporates physiological parameters such as blood flow and organ volume into the model.

This research aims to integrate a physiollogicaly based pharmacokinetic model (PBPK) with a bone remodeling model based on the dynamics of bone cells populations. The model of cells populations describes the signaling between osteoblasts and osteoclasts is based on the model of Lemaire et al. (2004), adding the mechanical stimulus proposed by Scheiner et al. (2013). The PBPK model will provide the concentration of the drug in bone making it possible to calculate a regulatory function that will influence the dynamics of bone cells population. The antiresorptive action of the drug is represented here by a loss of efficacy of active osteoclasts.

We simulate this effect in the model adding a regulatory function in the RANKL expression and increasing the osteoclasts apoptosis.

2 MATERIALS AND METHODS

2.1 Physiologically based pharmacokinetic model

A physiologically based pharmacokinetic model (PBPK) describes the drugs concentrations in blood and other organs using physiological parameters such as blood flow and organ volume as well as compartments representing different tissues and organs. A schematic of the PBPK model structure is given in Fig. 1. As can be seen in the model, the body is divided into a number of tissue compartments, each one characterized by appropriate volume and flow rates. For simplicity, we adopt the compartments blood, gut, liver, kidney, well perfused tissues, poorly perfused tissues and bone.

The bone compartment consists of two subcompartments: a rapidly exchangeable vascularized surface bone and an extravascularized bone matrix. The temporal evolution of the drug concentration in the tissue is described with a mass balance equation wich accounts for tissue blood flow rate (Q_i) and the concentration difference between the arterial blood (c_A) and the venous blood (c_{V_i}). Each tissue bone flow rate is assumed to be proportional to the cardiac output (Q_c) and based on reference values for a 70 Kg man (Yokley et al., 2006). Mean cardiac output is assumed to be 276 liters per hour. Physiological values are adjusted to satisfy the requirement $Q_c = \Sigma Q_i$ where i correspond to the tissues: gut, kidney, liver, rapid perfused, slowly perfused and bone. Volumes of each organ are considered fractions of body weight (BW) in $[Kg]$ as seen in Tab. 1.

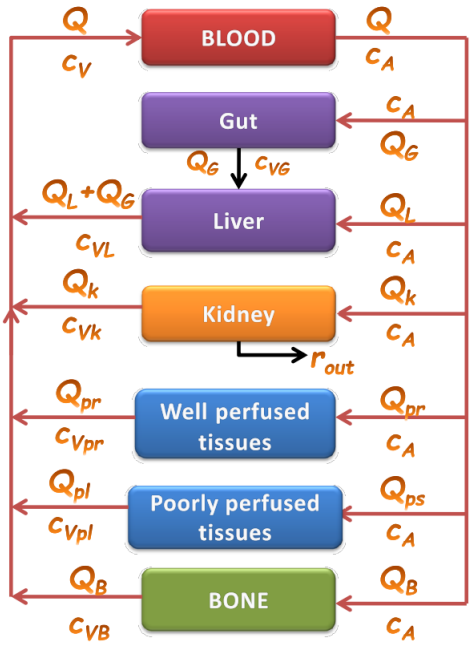

Figure 1: Physiologically based pharmacokinetic (PBPK) model. Q terms are blood flow rates, c terms are concentrations. Arterial input is on the right and venous effluent in on the left. Source: Prepared by the author.

Route of administration for a drug may be intravenous, usually as an injection or infusion, or oral, through the alimentary canal (gastrointestinal tract). In addition to these routes of administration, there are also pulmonary (inhalation), subcutaneous (adhesives), muscles (injection) and eyes (eye drops). Drugs administered orally may be absorbed in different parts of the gastrointestinal tract. Drugs absorbed through the oral cavity or rectum ignore the liver. All other parts of the alimentary canal (especially the stomach, duodenum, large and small intestine) carry blood (and drugs) in the liver through the portal vein. There are also transporters in the mucosal cells of the gut wall that pick up the drug from the gut and may excrete the drug back into the intestine. Relatively high drug concentrations are processed by the liver during the first passage of the drug. The liver can excrete the drug in the bile and then into the duodenum. Therefore, the drug can be resorbed resulting in a enterohepatic cycle (Gieschke and Serafin, 2013).

The main organs that undergo the drug elimination are the liver and the kidneys. The liver with its enzymatic equipment is the main metabolizing organ in the body. The kidneys help to filter wastes (including small drugs) from the blood and excrete them with urine. Absorption of the drug by tissue may be limited by blood perfusion or tissue permeability.

The mass balance equations for the PPPK model presented in the Fig. 1 is shown below. The variables V_i, c_i, Q_i are volume, concentration and blood flow in the tissue/organ i, respectively. The indices b, G, L, K, RP, SP, B refers to blood, gut, liver, kidney rapidly perfused tissues, slowly perfused tissues and bone, respectively.

$$V_b \frac{dc_b}{dt} = Q\left(c_V - c_A\right) + Dose(t) \qquad c_b\left(0\right) = 0 \tag{1}$$

$$V_G \frac{dc_G}{dt} = Q_G\left(c_A - c_{V_G}\right) \qquad c_G\left(0\right) = 0 \tag{2}$$

$$V_L \frac{dc_L}{dt} = Q_L c_A + Q_G c_{V_G} - \left(Q_L + Q_G\right) c_{V_L} \qquad c_L\left(0\right) = 0 \tag{3}$$

$$V_K \frac{dc_K}{dt} = Q_K\left(c_A - c_{V_K}\right) \qquad c_K\left(0\right) = 0 \tag{4}$$

$$V_{RP} \frac{dc_{RP}}{dt} = Q_{RP}\left(c_A - c_{V_{RP}}\right) \qquad c_{RP}\left(0\right) = 0 \tag{5}$$

$$V_{SP} \frac{dc_{SP}}{dt} = Q_{SP}\left(c_A - c_{V_{SP}}\right) \qquad c_{SP}\left(0\right) = 0 \tag{6}$$

$$V_B \frac{dc_B}{dt} = Q_B\left(c_A - c_{V_B}\right) \qquad c_B\left(0\right) = 0 \tag{7}$$

where:

$$c_A = c_b \quad c_{VG} = \frac{c_G}{R_G} \quad c_{VL} = \frac{c_L}{R_L} \quad c_{VK} = \frac{c_K}{R_K} \tag{8}$$

$$c_{V_{RP}} = \frac{c_{RP}}{R_{RP}} \quad c_{V_{SP}} = \frac{c_{SP}}{R_{SP}} \quad c_{V_B} = \frac{c_B}{R_B} \tag{9}$$

$$c_V = \frac{\left(Q_L + Q_G\right) c_{V_L} + Q_K c_{V_K} + Q_{RP} c_{V_{RP}} + Q_{SP} c_{V_{SP}} + Q_B c_{V_B}}{Q} \tag{10}$$

and finally the total blood flow is expressed by:

$$Q = Q_L + Q_G + Q_K + Q_{RP} + Q_{SP} + Q_B \tag{11}$$

Table 1: Physiological parameters used in the PBPK model.

Simbol	Unit	Value	Description	Source
Q_c	l/h	276	Cardiac output	Calculated
Q_{gut}	l/h	$0.19Q_c$	Blood flow to gut	Brown et al. (1997)
Q_{kidney}	l/h	$0.19Q_c$	Blood flow to gut	Brown et al. (1997)
Q_{liver}	l/h	$0.06Q_c$	Blood flow to gut	Brown et al. (1997)
Q_{bone}	l/h	$0.19Q_c$	Blood flow to gut	Brown et al. (1997)
Q_{rp}	l/h	$0.36Q_c$	Blood flow to well perfused tissues	Brown et al. (1997)
Q_{sp}	l/h	$0.125Q_c$	Blood flow to slowly/poorly perfused tissues	Calculated
V_{gut}	l	$0.2895BW$	Gut volume	Adapted from Pertinez et al. (2013)
V_{kidney}	l	$0.004BW$	Liver volume	Yokley et al. (2006)
V_{liver}	l	$0.025BW$	Kidney volume	Yokley et al. (2006)
V_{rp}	l	$0.04BW$	Well perfused tissues volume	Yokley et al. (2006)
V_{bone}	l	$0.04BW$	Bone volume	O'Flaherty (1991)
V_{sp}	l	4	Poorly perfused tissues volume	Calculated
R_{gut}	n/a	0.9	Partition coefficient gut/plasma	Pertinez et al. (2013)
R_{liver}	n/a	0.47	Partition coefficient liver/plasma	Pertinez et al. (2013)
R_{kidney}	n/a	3	Partition coefficient kidney/plasma	Pertinez et al. (2013)
R_{rp}	n/a	0.9	Partition coefficient well perf. tissues/plasma	Pertinez et al. (2013)
R_{sp}	n/a	0.6	Partition coefficient poorly perf. tissues/plasma	Pertinez et al. (2013)
$R_{bonesurface}$	n/a	2	Partition coefficient bone/plasma	Authors
CL_{renal}	l/h	0.03	Renal clearance	Pertinez et al. (2013)
CL_{hepato_bilis}	l/h	0.03	Renal clearance	Pertinez et al. (2013)

The PBPK model was implemented in Matlab. Physiological parameters were taken or derived from O'Flaherty (1991); Pertinez et al. (2013); Brown et al. (1997); Yokley et al. (2006) and are listed in Tab. 1. The drug concentration in bone at steady state define an input for the bone remodeling model based on cells activities.

Bone tissue modelling

The mineralized components of bone tissue are described by an adaptation of the permeability rate limited tissue compartment model (Nestorov, 2003; Pertinez et al., 2013). Thus, the bone compartment is composed by a vascular compartment that is taken as the bone surface and a extravascular as the bone matrix. The bone remodelling process will govern the exchange between these two compartments. Expressing in mathematical terms, the concentration in vascularized bone surface and extravascular bone matrix can be modelled by:

$$\frac{dA_{vas}}{dt} = \left(\frac{Q_{bone}c_A}{V_{vas}} - \frac{Q_{bone}A_{vas}}{V_{vas}R_{bone}}\right) - k_{form}\frac{A_{vas}}{V_{vas}} + k_{res}\frac{A_{bm}}{V_{bm}} \tag{12}$$

$$\frac{dA_{bm}}{dt} = k_{form}\frac{A_{vas}}{V_{vas}} - k_{res}\frac{A_{bm}}{V_{bm}} \tag{13}$$

The terms k_{form} and k_{res} describes the bone formation and bone resorption rates, respectively, and are both defined in the bone cells populations model. Fig. 2 ilustrates the model for the bone tissue.

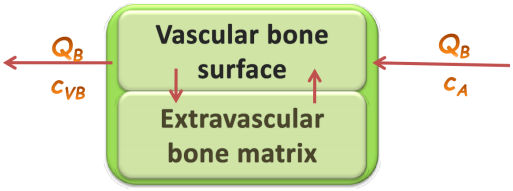

Figure 2: Bone tissue compartment model.

2.2 Cells populations model

Lemaire *et al.* (Lemaire et al., 2004) proposes a mathematical model to describe the dynamics of bone cells populations (pre-osteoblasts, active osteoblasts and active osteoclasts) during the bone remodeling. The model includes the osteoblast-osteoclast coupling, RANK-RANKL-OPG signaling, allows to simulate some bone metabolic diseases and also the antagonistic effects of PTH administration.

The Lemaire et al. (2004) model considers four steps in the development of osteoblasts: precursors, responsive, active and a fourth group that aggregates apoptotic cells and osteocytes. In the case of non-committed precursors, they form a reservoir with a constant amount of cells that can be differentiated into osteoblasts responsive to the influence of a stimulatory factor on the differentiation process such as the $TGF-\beta$ protein. This protein also acts on the responsible osteoblasts preventing differentiation of these into the next step. Active osteoblasts are influenced by PTH in the control of the production of OPG and RANKL (Daniel, 2013).

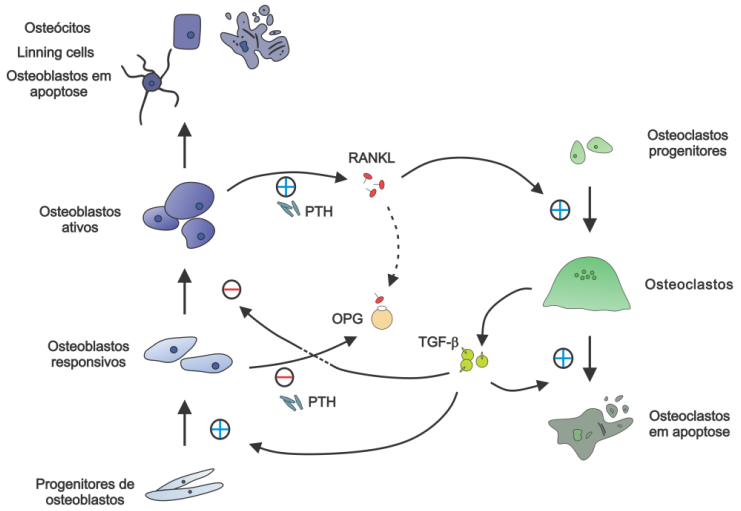

Figure 3: Diagrammatic representation of the basic structure of the Lemaire's model (Lemaire et al., 2004). Source: Mercuri (2013)

RANKL induces the differentiation of active osteoclasts which release $TGF-\beta$ causing osteoclastic apoptosis and the control of osteoblast differentiation. A graphical scheme of the model is presented in Fig. 3.

The behavior of bone cells is regulated when receptors located on the cells surface are activated by cytokines, produced by other cells or by itself. The chemical kinetics of reactions can be represented by the law of mass action. The original model proposed by Lemaire et al. (2004), does not include the contribution of mechanical stimuli and the action of an antiresorptive agent [1].

In the present work, both the mechanical stimuli proposed by Scheiner et al. (2013) and the action of an antiresorptive agent (Ross et al., 2017), such as bisphosphonate, are included. The drug concentration in bone obtained by the PBPK model will be used here to evaluate a pharmacoregulation function for the dynamic of the bone cells population.

In mathematical terms, the temporal evolution of bone cells can be expressed by the system of ordinary differential equations shown below, Eqs. 14-18. The variables OB_p, OB_a and OC_a refers to pre-osteoblasts, active osteoblasts and active osteoclasts, respectively. The variables BA and BM are the antiresorptive drug concentration in the bone matrix and the biomarker for bone mineral density (BMD), respectively. In this way, the following system of ordinary differential equations is obtained:

$$\frac{dOB_p}{dt} = D_R\pi_C + P_{OB_p}OB_p\Pi_\varepsilon - \frac{D_B}{\pi_C}\cdot OB_p \tag{14}$$

$$\frac{dOB_a}{dt} = \frac{D_B}{\pi_C}OB_p - k_BOB_a \tag{15}$$

$$\frac{dOC_a}{dt} = D_C\pi_L - (1+k_7BA)D_A\pi_COC_a \tag{16}$$

$$\frac{dBA}{dt} = k_8BI(1-BA) - k_9BA \tag{17}$$

$$\frac{dBM}{dt} = k_{10}\left(\frac{OB_a}{OC_a} - k_{12}\right) - k_{11}(BM-1) \tag{18}$$

where D_B is a factor of proportionality and π_C is the influence of $TGF-\beta$, expressed by:

$$D_B = f_0d_B\pi_C = \frac{C+f_0C^S}{C+C^S} \tag{19}$$

The RANKL influence, π_L is obtained by:

$$\pi_L = \frac{k_3}{k_4}\frac{K_L^P.\pi_P.B}{1+\frac{k_3}{k_4}+\frac{k_1}{k_2k_0}\left(\frac{K_O^P}{\pi_P+I_0}\right)}\left(1+\Pi_{BA}+\frac{I_L+P_{RL_{\varepsilon_{bm}}}}{r_L}\right) \tag{20}$$

where π_P is the fraction of occupied PTH receptors which is expressed by:

$$\pi_P = \frac{\frac{I_P}{k_P}+\frac{S_P}{k_P}}{\frac{I_P}{k_P}+\frac{k_6}{k_5}} \tag{21}$$

and BI is the concentration of anti-resorptive drug in plasma. The term $P_{RL_{\varepsilon_{bm}}}$ corresponds

[1] Drugs used for treatment and prevention of osteoporosis can be divided basically into two categories : anti-resorptive agents or anabolic agents. Anti-resorptive agents reduce bone resorption, leading to increased BMD by several degrees. Estrogen, raloxifene, bisphosphonates and the human monoclonal antibody to RANKL are included in this category. On the other hand, anabolic agents such as teriparatide (PTH1-34) and total parathyroid hormone (PTH1-84), stimulate bone formation, thus increasing BMD (Szulc and Bouxsein, 2011).

to the variation of the RANKL related to changes in the energy density of deformation, only activated in the disuse and expressed by:

$$P_{RL_{\varepsilon_{bm}}} = \kappa \left(1 - \frac{w_{\varepsilon_{bm}}}{w_{\varepsilon_{bm_{st}}}}\right) \tag{22}$$

where the adjustement constant κ is null for $w_{\varepsilon_{bm}} \geq w_{\varepsilon_{bm_{st}}}$. and positive otherwise.

The term Π_{BA} is a drug-regulatory function which simulates the effect of the external administration of an antiresorptive drug on the population of cells. The term was added in the original expression proposed by Lemaire et al. (2004) for the RANKL concentration equation, being expressed by:

$$\Pi_{BA} = k_{BA} BA \tag{23}$$

where BA is the concentration of the antiresorptive drug in the bone matrix taken from PBPK model and k_{BF} is an adjustment constant for the model.

The population of preosteoblasts OB_p increases with the differentiation of progenitor osteoblast cells with a maximal differentiation rate D_R, promoted by the growth factor $TGF-\beta$. On the other hand, the population of precursor osteoblasts decreases due to the differentiation of the precursor osteoblasts into active osteoblasts which occurs at a maximum rate.

Following the proposal of Scheiner et al. (2013) the mechanical stimulus is modeled adding a term in Eq. 14 by regulating the proliferation of osteoblasts as a function of the value of the locally evaluated deformation energy density. The function Π_ε is the mechanoregulation and P_R is the constant indicating the proliferation of osteoblasts according to the strain energy density:

$$\Pi_\varepsilon = \Pi_{\varepsilon_{st}} \left(1 + \lambda \left(\frac{w_{\varepsilon_{bm}}}{w_{\varepsilon_{bm_{st}}}} - 1\right)\right) \tag{24}$$

where $\Pi_{\varepsilon_{st}}$ is the equilibrium value of Π_ε, $w_{\varepsilon_{bm}}$ is the value of local strain energy density and $w_{\varepsilon_{bm_{st}}}$ is the equilibrium value. Parameter λ is an adjustement constant which is null to $w_{\varepsilon_{bm}} \leq w_{\varepsilon_{bm_{st}}}$ and positive otherwise.

The active osteoblast population OB_a is increased according to the pre-osteoblast differentiation that occurs with the maximum differentiation rate D_B which is inhibited by the $TGF-\beta$. The population is reduced by the apoptosis of active osteoblasts which occurs with rate of apoptosis k_B.

Antiresorptive drugs such as bisphosphonates bind to the hydroxyapatite in the bone and inhibit its reabsorption by osteoclasts. In the model the loss of efficacy of osteoclasts is simulated by a change in RANKL concentration in Eq. 20 and by an increase in the rate of apoptosis of active osteoclasts in Eq. 16. The bisphosphonate attaches to the bone in a second-order forward, first-order reverse reaction with hydroxyapatite attachment sites, (Ross et al., 2017), providing values between $[0, 1]$:

According to Ross et al. (2017), the model uses bone mineral density (BMD) as a reference biomarker, denoting BMD in the Eq. 18. Considering that the term that underlies BMD is the osteoblast/osteoclast ratio, it is incorporated into the system of differential equations including a ratio between the difference of the osteoblast/osteoclast ratio and its reference value. In the absence of treatment the biomarker for BMD returns to the baseline value 1.

The model parameters are summarized in Table 2

Table 2: Parameters used in the simulation of the bone remodeling model. Values extracted from Refs. Lemaire et al. (2004) except $k_i(i = 7, ..., 12)$ and k_{BA} adjusted by the authors

Symbol	Value	Description
$C^s[pM]$	5×10^{-3}	Number of OC to get half differentiation flux
$D_A[dia^{-1}]$	0.7	Rate of osteoclast apoptosis caused by $TGF - \beta$
$d_B[dia^{-1}]$	0.7	Differentiation rate of responding osteoblasts
$D_C[pM.dia^{-1}]$	2.1×10^{-3}	Differentiation rate of osteoclast precursors
$D_R[pM.dia^{-1}]$	7×10^{-4}	Differentiation rate of osteoblast progenitors
f_0	0.05	Fixed proportion
$I_L[pM.dia^{-1}]$	$0 - 10^6$	Rate of administration of RANKL
$I_O[pM.dia^{-1}]$	$0 - 10^6$	Rate of administration of OPG
$I_P[pM.dia^{-1}]$	$0 - 10^6$	Rate of administration of PTH
$K[pM]$	10	Fixed concentration of RANK
$k_1[pM^{-1}.dia^{-1}]$	10^{-2}	Rate of OPG-RANKL binding
$k_2[dia^{-1}]$	10	Rate of OPG-RANKL unbinding
$k_3[pM^{-1}.dia^{-1}]$	5.8×10^{-4}	Rate of RANK-RANKL binding
$k_4[pM.dia^{-1}]$	1.7×10^{-2}	Rate of RANK-RANKL unbinding
$k_5[pM^{-1}.dia^{-1}]$	0.02	Rate of PTH binding with its receptor
$k_6[dia^{-1}]$	3	Rate of PTH unbinding
$k_B[dia^{-1}]$	0.189	Rate of elimination of active osteoblasts
$K_L^P[pmol/pmol]$	3×10^6	Maximum RANKL attached on each cell surface
$k_O[dia^{-1}]$	0.35	Rate of elimination of OPG
$K_O^P[dia^{-1}]$	2×10^5	Minimal rate of production of OPG per cell
$k_P[dia^{-1}]$	86	Rate of elimination of PTH
$r_L[pM.dia^{-1}]$	10^3	Rate of RANKL production and elimination
$S_P[pM.dia^{-1}]$	250	Rate of synthesis of systemic PTH
$\lambda[adim]$	1.2	Parameter of anabolic adjustment
$\kappa[adim]$	5×10^2	Parameter of RANKL inibition
$\Pi_{\varepsilon_{st}}[adim]$	0.5	Equilibrium of mechanoregulation function
$w_{\varepsilon_{bm_{st}}}[Pa]$	0.78	SED inferior limit
$k_7[adim]$	0.3	Hill function parameter for apoptosis of OC_a
$k_8[pM.dia^{-1}]$	6×10^{-3}	Bisphosphonate transfer from plasma to bone
$k_9[1/h]$	5×10^{-4}	Bisphosphonate on bone clearance rate
$k_{10}[1/h]$	25×10^{-5}	First order BMD rate OC_a/OB_a
$k_{11}[1/h]$	1.5×10^{-4}	BMD equilibration
$k_{12}[adim]$	$0,7979$	Baseline value of the OC_a/OB_a
$k_{BA}[adim]$	1	Parameter of the Hill function for drug regulation

2.3 Finite Elements Model

In order to apply the proposed procedure, a finite element model was built from CT images of an osteoporotic femur. The initial densities were accessed from the CT images and transferred to the FEM model, as shown in Fig. 5. A linear relation between the grayscale pixels values $[0.255]$ and the bone densities was adopted.

There are in the scientific literature several relations between Young's modulus and apparent bone densities (Carter and Hayes, 1977; Morgan et al., 2003; Snyder and Schneider, 1991; Kaneko et al., 2004; Keller, 1994). A review of studies in this area can be found in the work of Helgason et al. (2008). Some of the established relationships are illustrated in Fig. 4.

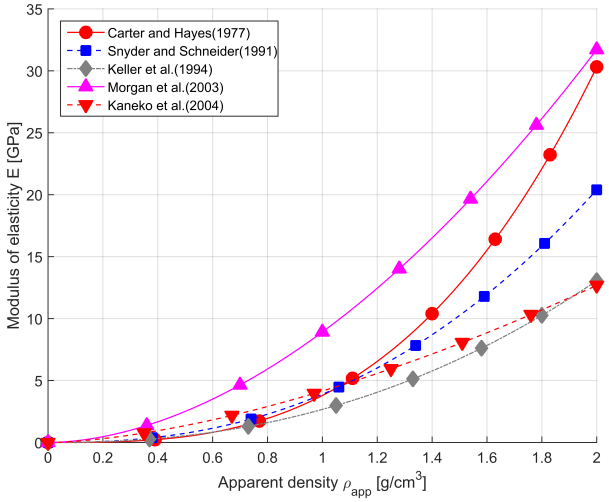

Figure 4: Examples of relationships between modulus of elasticity and apparent density available in the literature. Source: Prepared by the author.

Here the elasticity modulus is evaluated as a function of the ash densities using the relation proposed by Keller (1994) and validated by (Yosibash et al., 2007) and (Trabelsi et al., 2009):

$$E_{cort} = 10200\rho_{ash}^{2.01}\,[MPa] \tag{25}$$

$$E_{trab} = 5307\rho_{ash} + 469\,[MPa] \tag{26}$$

In order to distinguish the trabecular and cortical bone types, the condition $\rho_{ash} > 0.6g/cm^3$ to cortical bone and $\rho_{ash} \leq 0.6g/cm^3$ for trabecular bone, were adopted as proposed by Trabelsi et al. (2014).

The model was fully implemented in Matlab with post-processing in Paraview 5.0.0. The procedure for reconstruction and mapping of non-homogeneous isotropic material properties is described in more details in the work of Bahia et al. (2016).

The hip joint model of Nedoma and Stehlik (2011) was adapted to define the pressure values in the femoral head (adductor forces) and in the large trochanter (abductor forces). The forces acting on the femur (Nedoma and Stehlik, 2011) were obtained from static equilibrium conditions considering a person of 800 N. An adductor force acting on the femoral head of 1920 N was taken to form $16.^\circ$ with the sagittal plane and an abductor force of 1850 N at an angle of 22°. The forces were proportionally distributed at the nodes of the femoral head and at the large trochanter as shown in Fig. 7. The nodes of the lower part of the femur were held fixed.

Thus the bone cells populations model was implemented incorporating a finite element structural analysis algorithm for the three-dimensional case. Thus, each interaction of the structural analysis calculates the local strain energy density for each node of the discretized mesh. Therefore, the system of differential equations that govern the temporal evolution of the bone

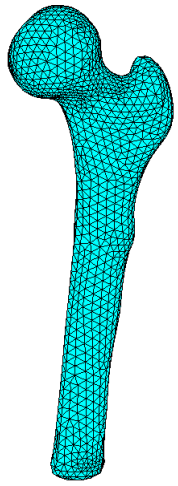

Figure 5: Discretization of the reconstructed femur in a finite element mesh with 3846 nodes and 16689 tetrahedral elements. Source: Prepared by the author.

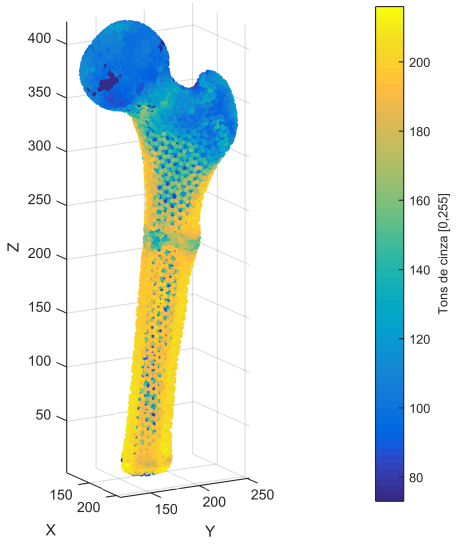

Figure 6: Assignment of gray values in mesh elements. Source: Prepared by the author.

cell populations is solved. A new cells population is calculated at each node and the bone mass is updated at each iteration.

3 Preliminary results

This work proposes an unified model for bone remodeling, including the dynamics of bone cell populations and a pharmacokinetic model. The overall diagram of the proposed procedure is shown in Fig. 8.

The implementation of the PBPK model generated the graph shown in Fig. 9. The physiological parameters used in the simulation are listed in Tab. 1. A dosing regimen of antiresorptive drug (12 mg for 4h) via intravenous infusion was adopted in this simulation.

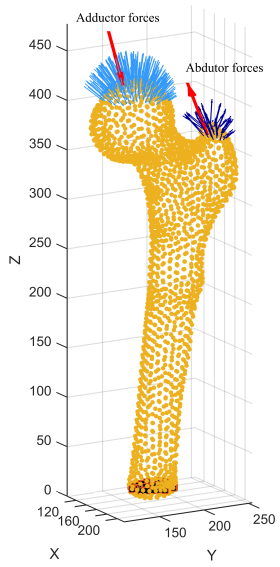

Figure 7: Boundary conditions applied to the FEM model. Source: Prepared by the author.

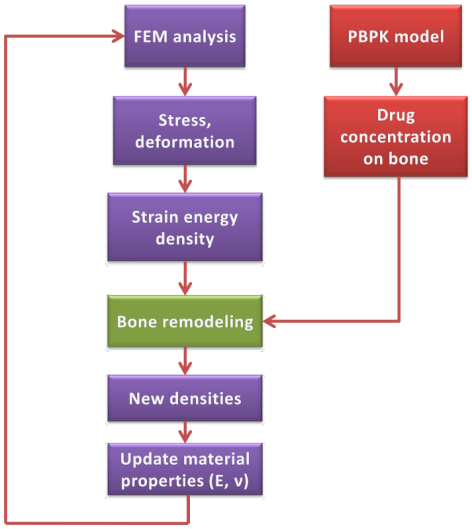

Figure 8: Diagram for the proposed unified bone remodeling model. A pharmacokinetic model provides the plasma concentration of the drug that contributes to the evolution of bone cells populations. Source: Prepared by the author.

The bone cells populations model represented by Eqs. 14-18 is ilustrated on Figs. 10 and 11. The model was analyzed through numerical integration with the $4th$ order Runge-Kutta algorithm programmed in Matlab. In the first simulation illustrated in Fig. 10 a strain energy density of 0.18 Pa was employed with no bisphosphonate stimulation. Approximately after $180th$ day of iteration the cells population of preosteoblasts, active osteoblasts and osteoclasts reach the steady state condition. At the end of 200 days the BMD biomarker had an increase of 2.57%.

The second simulation investigates the impact of adding an antireabsortive agent stimulus in bone cells population and BMD biomarker, as shown in Fig. 11. The mechanical stimulus was mantained equal to the first simulation but an antiresorptive agent stimulus was added.

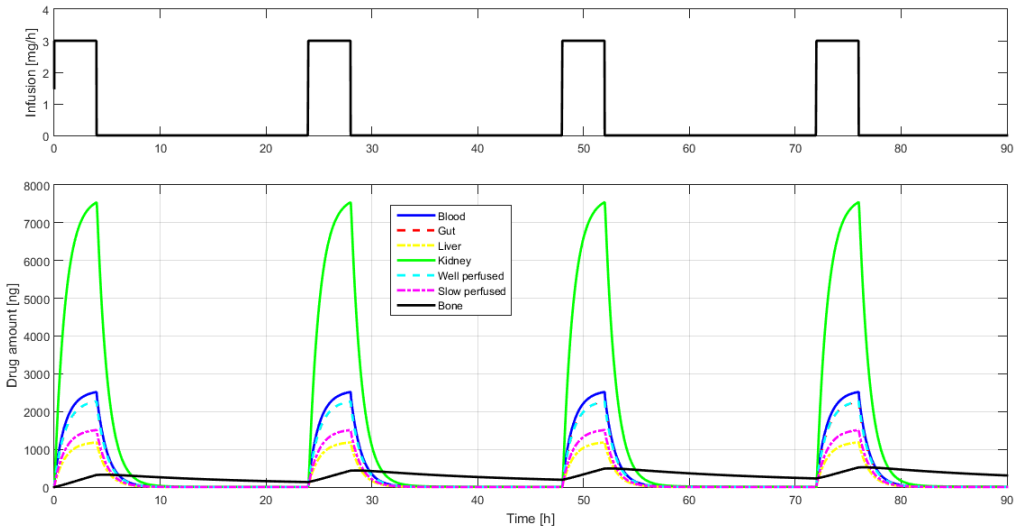

Figure 9: Time course of drug concentrations in body obtained with the PBPK model. Antiresorptive therapy with dosing regimen of 12 mg for 4 h via intravenous infusion was adopted. A Heaviside function represents in mathematical terms the drug administration. Source: Prepared by the author.

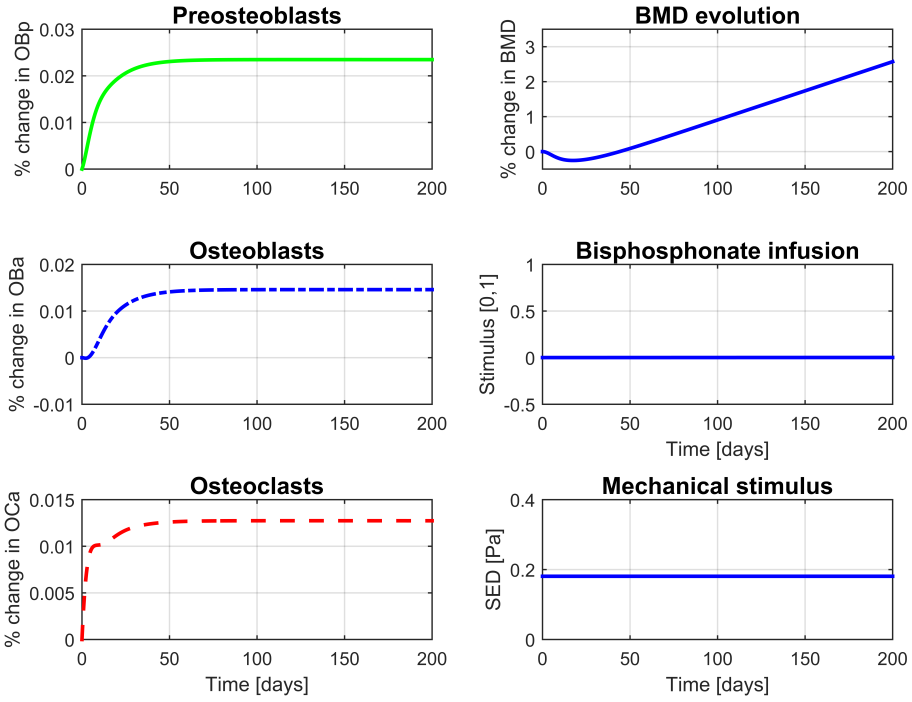

Figure 10: Effect of mechanical stimulation on bone mineral density. Simulation of the Lemaire model for the temporal evolution of bone populations of precursor osteoblasts (OB_p), active osteoblasts (OB_a) and active osteoclasts (OC_a). Mechanical stimulus promoted by strain energy density (SED). Source: Prepared by the author.

The antiresorptive effect was reproduced in the model with an increase in the rate of active

osteoclast apoptosis and the inclusion of a regulatory function in RANKL expression. Using the same simulation parameters except for the inclusion of antiresorptive agent stimulus after $20th$ day, we observed an BMD increase of 3.20%, slightly higher than that obtained in the previous simulation.

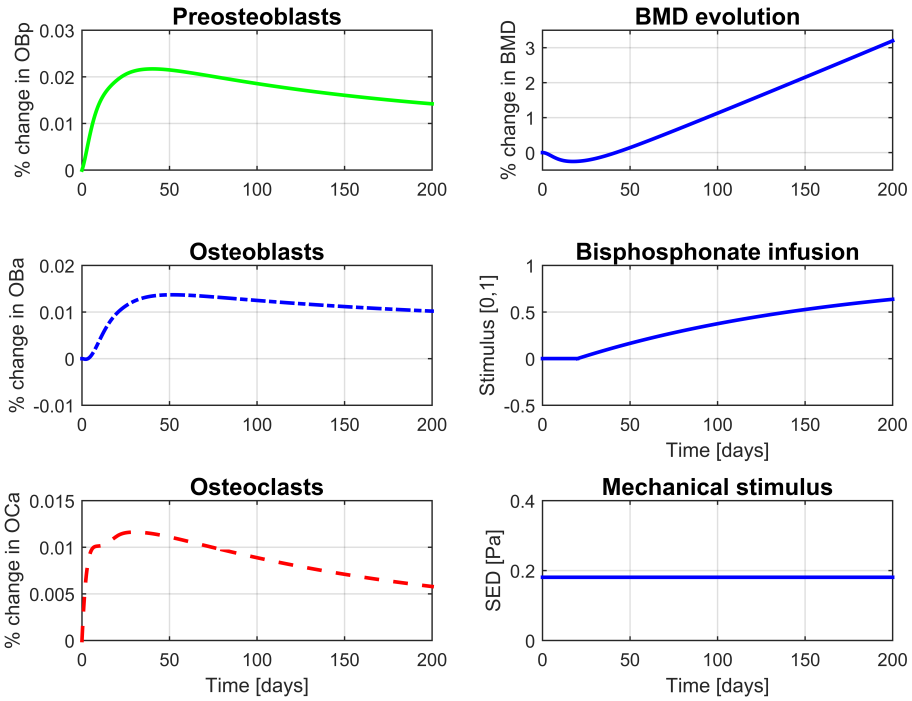

Figure 11: Effect of mechanical stimulation on bone mineral density. Simulation of the Lemaire model for the temporal evolution of bone populations of precursor osteoblasts (OB_p), active osteoblasts (OB_a) and active osteoclasts (OC_a). Mechanical stimulus promoted by strain energy density (SED). Source: Prepared by the author.

The expression specifying the differentiation of pre-osteoblasts is a function of the concentration of active osteoclasts. Thus, only increasing apoptosis of active osteoclasts does not result in an increase in the population of active osteoblasts, but rather reduces the rate of differentiation of precursor osteoblasts. The increase in the osteoclast osteoblast ratio was obtained by modifying RANKL expression with the inclusion of the drug-regulatory function, Eq. 23, in the Eq. 20.

Each iteration of the procedure involves a structural analysis by the finite element method, numerical integration of the system of differential equations that governs the dynamics of cellular populations and update of mechanical properties. The temporal evolution of the cell populations is performed in cycles of 120 days. Figure 12 shows the distribution of densities in a longitudinal section of the reconstructed femur for initial and final configurations after 4 iterations or 480 days.

Fig. 13 ilustrates a cross section of the femur in the diaphyseal region after the convergence of the algorithm. An approximate increase in the cortical bone area of 7.68% was observed comparing to the initial area. This value was estimated through an image segmentation using the *K*-means clustering algorithm and subsequent counting of the number of pixels of segmented

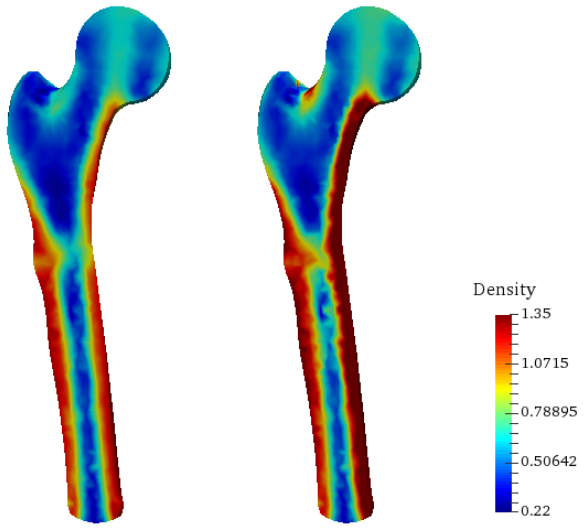

Figure 12: Densities distribution in the femur. Initial (left) and final configurations (right) after 480 days. Source: Prepared by the author.

regions (adding areas 1 and 2 shown in the Fig. 13). Convergence of the algorithm can be visualised in Fig. 14

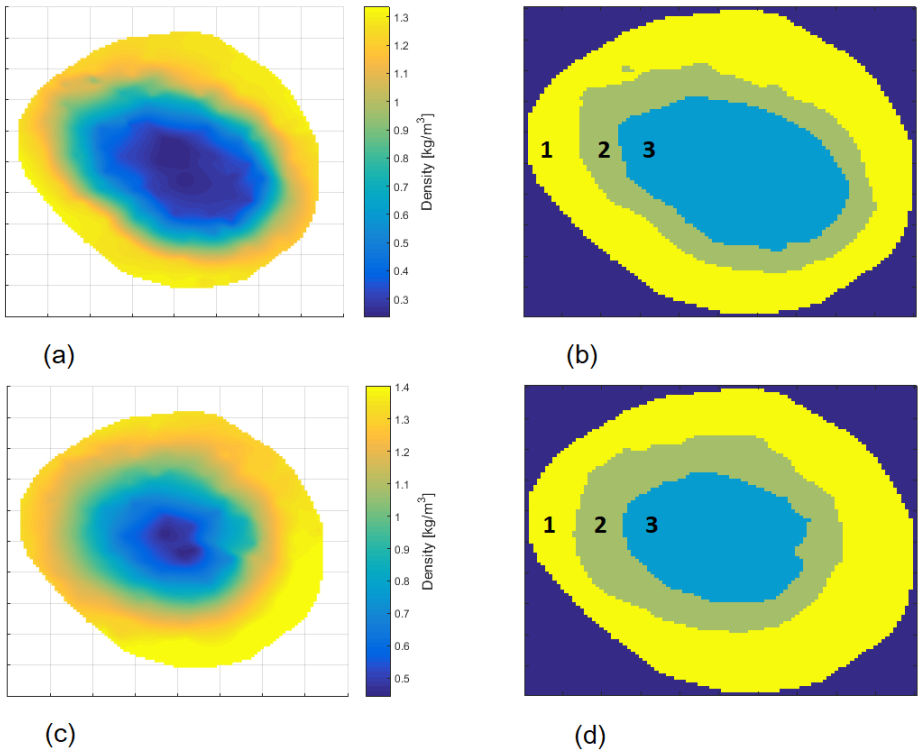

Figure 13: Cross section of the femur in the diaphyseal region: (a) initial densities distribution, (b) segmentation of cortical region (adding areas 1 and 2), (c) final densities distribution after convergence of the procedure and (d) cortical region after convergence. Image segmentation using K-means clustering algorithm was adopted to evaluate the percentage increase of the cortical region. Source: Prepared by the author.

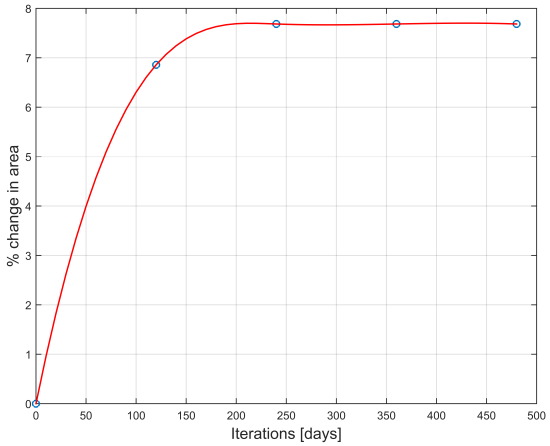

Figure 14: Convergence of the algorithm after approximately 360 iterations. Source: Prepared by the author.

Preliminary results from the research indicated that the model captures qualitatively well the adaptive behavior of bone and cellular interactions during remodeling. The increase in the rate of apoptosis of osteoclasts simultaneously produces a decrease in the rate of differentiation of pre-osteoblasts. Therefore, the anti-resorptive action should not be based solely on the increase in the rate of osteoclastic apoptosis as this is not sufficient to represent an increase in BMD obtained with drug administration. This desired effect was obtained with a modification in RANKL expression including a regulatory function corresponding to the presence of medicament. Additional efforts should be employed to calibrate model parameters to better replicate the behavior of commercially available antiresorptive medications for the treatment of osteoporosis such as alendronate, risedronate, among others. The measurement of the increase in the area for cortical bone through image segmentation using K-means clustering algorithm allowed a practical quantitative evaluation of the effectiveness of the procedure.

ACKNOWLEDGEMENTS

The authors would like to acknowledge Dr. Marcelo de Medeiros Pinheiro of the Department of Medicine of the Universidade Federal de São Paulo (UNIFESP) for kindly donate the CT images used in this work.

REFERENCES

Bahia, M. T., Mercuri, E. G., and Hecke, M. B. (2016). Fe analyses of a reconstructed femur with mapping of inhomogeneous isotropic material properties from ct images. In *Proceedings of the VII European Congress on Computational Methods in Applied Sciences and Engineering*, Crete Island, Greece.

Brown, R. P., Delp, M. D., Lindstedt, S. L., Rhomberg, L. R., and Beliles, R. P. (1997). Physiological parameter values for physiologically based pharmacokinetic models. *Toxicology and industrial health*, 13(4):407–484.

Carter, D. R. and Hayes, W. C. (1977). The compressive behavior of bone as a two-phase porous structure. *The Journal of Bone & Joint Surgery*, 59(7):954–962.

Daniel, A. L. (2013). Um modelo mecanobiológico multiescala para remodelamento ósseo. Master's thesis, Universidade Federal do Paraná, Curitiba, Brasil.

Gieschke, R. and Serafin, D. (2013). *Development of innovative drugs via modeling with MATLAB*. Springer.

Hambli, R., Boughattas, M. H., Daniel, J.-L., and Kourta, A. (2016). Prediction of denosumab effects on bone remodeling: A combined pharmacokinetics and finite element modeling. *Journal of the mechanical behavior of biomedical materials*, 60:492–504.

Helgason, B., Perilli, E., Schileo, E., Taddei, F., Brynjólfsson, S., and Viceconti, M. (2008). Mathematical relationships between bone density and mechanical properties: a literature review. *Clinical biomechanics*, 23(2):135–146.

Kaneko, T. S., Bell, J. S., Pejcic, M. R., Tehranzadeh, J., and Keyak, J. H. (2004). Mechanical properties, density and quantitative ct scan data of trabecular bone with and without metastases. *Journal of biomechanics*, 37(4):523–530.

Keller, T. S. (1994). Predicting the compressive mechanical behavior of bone. *Journal of biomechanics*, 27(9):1159–1168.

Komarova, S. V., Smith, R. J., Dixon, S. J., Sims, S. M., and Wahl, L. M. (2003). Mathematical model predicts a critical role for osteoclast autocrine regulation in the control of bone remodeling. *Bone*, 33(2):206–215.

Kroll, M. H. (2000). Parathyroid hormone temporal effects on bone formation and resorption. *Bulletin of mathematical biology*, 62(1):163–188.

Lemaire, V., Tobin, F. L., Greller, L. D., Cho, C. R., and Suva, L. J. (2004). Modeling the interactions between osteoblast and osteoclast activities in bone remodeling. *Journal of theoretical biology*, 229(3):293–309.

Mercuri, E. G. F. (2013). *Modelagem multiescala de tecidos mineralizados considerando a micromecânica da dinâmica celular*. PhD thesis, Universidade Federal do Paraná, Curitiba, Brasil.

Morgan, E. F., Bayraktar, H. H., and Keaveny, T. M. (2003). Trabecular bone modulus–density relationships depend on anatomic site. *Journal of biomechanics*, 36(7):897–904.

Mori, T. and Tanaka, K. (1973). Average stress in matrix and average elastic energy of materials with misfitting inclusions. *Acta metallurgica*, 21(5):571–574.

Nedoma, J. and Stehlik, J. (2011). *Mathematical and Computational Methods and Algorithms in Biomechanics: Human Skeletal Systems*, volume 12. John Wiley & Sons.

Nestorov, I. (2003). Whole body pharmacokinetic models. *Clinical pharmacokinetics*, 42(10):883–908.

O'Flaherty, E. J. (1991). Physiologically based models for bone-seeking elements: Iii. human skeletal and bone growth. *Toxicology and applied pharmacology*, 111(2):332–341.

Pertinez, H., Chenel, M., and Aarons, L. (2013). A physiologically based pharmacokinetic model for strontium exposure in rat. *Pharmaceutical research*, 30(6):1536–1552.

Pivonka, P., Zimak, J., Smith, D. W., Gardiner, B. S., Dunstan, C. R., Sims, N. A., Martin, T. J., and Mundy, G. R. (2008). Model structure and control of bone remodeling: a theoretical study. *Bone*, 43(2):249–263.

Rieger, R. (2011). *Modélisation mécano-biologique par éléments finis de l'os trabéculaire: des activités cellulaires au remodelage osseux*. PhD thesis, Université d'Orléans, Orléans, France.

Ross, D. S., Mehta, K., and Cabal, A. (2017). Mathematical model of bone remodeling captures the antiresorptive and anabolic actions of various therapies. *Bulletin of mathematical biology*, 79(1):117–142.

Scheiner, S., Pivonka, P., and Hellmich, C. (2013). Coupling systems biology with multiscale mechanics, for computer simulations of bone remodeling. *Computer Methods in Applied Mechanics and Engineering*, 254:181–196.

Scheiner, S., Pivonka, P., Smith, D., Dunstan, C., and Hellmich, C. (2014). Mathematical modeling of postmenopausal osteoporosis and its treatment by the anti-catabolic drug denosumab. *International journal for numerical methods in biomedical engineering*, 30(1):1–27.

Snyder, S. M. and Schneider, E. (1991). Estimation of mechanical properties of cortical bone by computed tomography. *Journal of Orthopaedic Research*, 9(3):422–431.

Szulc, P. and Bouxsein, M. L. (2011). Overview of osteoporosis: Epidemiology and clinical management. *Vertebral Fracture Initiative Resource Document PART I*.

Trabelsi, N., Milgrom, C., and Yosibash, Z. (2014). Patient-specific fe analyses of metatarsal bones with inhomogeneous isotropic material properties. *Journal of the mechanical behavior of biomedical materials*, 29:177–189.

Trabelsi, N., Yosibash, Z., and Milgrom, C. (2009). Validation of subject-specific automated p-fe analysis of the proximal femur. *Journal of biomechanics*, 42(3):234–241.

Yokley, K., Tran, H. T., Pekari, K., Rappaport, S., Riihimaki, V., Rothman, N., Waidyanatha, S., and Schlosser, P. M. (2006). Physiologically-based pharmacokinetic modeling of benzene in humans: a bayesian approach. *Risk Analysis*, 26(4):925–943.

Yosibash, Z., Trabelsi, N., and Milgrom, C. (2007). Reliable simulations of the human proximal femur by high-order finite element analysis validated by experimental observations. *Journal of biomechanics*, 40(16):3688–3699.